remote sensing

MDPI

Article

Residual Ash Mapping and Coffee Plant Development Based on Multispectral RPA Images

Lucas Santos Santana [1], Gabriel Araújo e Silva Ferraz [2,*], Mozarte Santos Santana [3], Nicole Lopes Bento [2], Josiane Maria da Silva [4] and Rafael de Oliveira Faria [2]

[1] Institute of Agricultural Sciences, Federal University of Vales do Jequitinhonha e Mucuri (UFVJM), Av. Universitária, P.O. Box 1000, Unaí 38610-000, Brazil; santana.santos@ufvjm.edu.br
[2] Agricultural Engineering Department, Federal University of Lavras (UFLA), P.O. Box 3037, Lavras 37200-900, Brazil; nicolelbento@gmail.com (N.L.B.); rafael.faria@ufla.br (R.d.O.F.)
[3] Institute of Natural Sciences, Federal University of Lavras (UFLA), P.O. Box 3037, Lavras 37200-900, Brazil; mozartesantana@outlook.com
[4] Forest Department, Federal University of Lavras (UFLA), P.O. Box 3037, Lavras 37200-900, Brazil; josiane.engflorestal@gmail.com
* Correspondence: gabriel.ferraz@ufla.br

Abstract: Residues mapping can provide essential information about soil chemical elements' behaviors and contribute to possible interferences in coffee tree development. Thus, the research objective was to monitor plant residue burning effects by analyzing the chemical elements in ash, using soil analysis, and applying vegetative indices obtained by RPA images. The samples were submitted for conventional soil analysis and atomic emission spectrometry (pure ash). The RPA multispectral images were used to form thirty-one vegetative indices. Thus, at the soil and ash collection points, the index performance was evaluated for six months and divided into three collection times. Then, the data were statistically analyzed to evaluate which index best separated the plants in regions with ash and ash-free soil. The pure ash deposits revealed expressive presences of K, Ca, Mg, and Al in addition to pH elevation. In areas with ash, the high temperature at the burning time may have caused elemental chemical transformations in the Al composition, making this element unavailable in soil analysis. The vegetative indices showed a significant difference only in coffee four months after planting. Among the thirty-one evaluated indices, only twenty were satisfactory for ash analysis. The burning of plant residues promoted the neutralization of Al. In addition, ash deposits in the soil added some essential elements for plant development. Negatively, they raised the PH and made micronutrients unavailable. The best vegetative indices for ash monitoring were the Normalized Near Infrared Index (NNIRI) and Normalized Green Index (NGI). Prior ash mapping can contribute to localized application in macro, such as K and limestone, reusing the number of elements already deposited by burning vegetables.

Keywords: precision agriculture; remote sensing; sustainability; soil management; coffee farm

check for updates

Citation: Santana, L.S.; Ferraz, G.A.e.S.; Santana, M.S.; Bento, N.L.; Silva, J.M.d.; Faria, R.d.O. Residual Ash Mapping and Coffee Plant Development Based on Multispectral RPA Images. *Remote Sens.* **2024**, *16*, 1917. https://doi.org/10.3390/rs16111917

Academic Editor: Kevin Tansey

Received: 12 April 2024
Revised: 21 May 2024
Accepted: 22 May 2024
Published: 27 May 2024

Copyright: © 2024 by the authors. Licensee MDPI, Basel, Switzerland. This article is an open access article distributed under the terms and conditions of the Creative Commons Attribution (CC BY) license (https://creativecommons.org/licenses/by/4.0/).

1. Introduction

Coffee growing represents an essential source of income for many countries [1,2]. Applying techniques that make agricultural production more efficient is essential [3,4]. Technological advances in coffee cultivation have contributed to obtaining accurate and reliable measurements for crop monitoring [5]. This makes intelligent agricultural practices crucial for maximizing yields and conserving natural resources [6,7].

Emerging technologies, such as remotely piloted aircraft systems (RPAs), substantially contribute to the significant development of agriculture [8,9]. Coffee-growing mapping areas by RPAs were applied to identify frost damage [10], determine biophysical parameters of coffee [6,11], and develop a method to detect coffee rust [12]. All these papers proved

RPA technology applicability in coffee-growing areas, but none addressed ash in the soil and its effects on coffee plant development.

Precision coffee growing presents technological developments offering several monitoring possibilities. Applications of RPAs in coffee-growing areas provide opportunities for mapping components present on the soil surface. Soil mapping possibilities by RPAs are evidenced in research on sustainable agriculture [13], soil monitoring for irrigation management [14], soil salinity [15], and soil plant dynamics and the environment [16]. The advantage of remote sensing technologies is that they offer highly assertive monitoring possibilities [17].

In some cases, cutting, molding, and burning plant biomass are used to renovate coffee-growing areas. Biomasses are combustible organic materials containing carbon, hydrogen, oxygen, minerals, and moisture [18]. Typically, woody materials, nonwoody agricultural waste, aquatic biomass, process waste, municipal solid waste, and animal and industrial waste are included [19]. Biomass combustion produces ash composed of elemental oxides, SiO_2, CaO, and K_2O, usually forming >60% ash from the virgin biomass. Ashes from biomass-containing residues typically contain more Al_2O_3 and Fe_2O_3 than ash from virgin biomasses [20]. The ashes can be used for soil fertilization in agriculture [21].

In coffee growing, one of the forms of management promotes ash deposits, which are formed by agricultural residues with a significant volume of biomass. Traditional techniques incorporate all these residues into the soil to contribute to subsequent plantation fertilization. Plant growth on agricultural waste is used in various crops [22]. In this form of management, crop residues are burned to renew the stand, forming visible areas of ash in the soil. Knowledge of techniques for efficiently using chemical elements deposited by burning biomass is essential to maximize environmentally safe alternatives and to achieve sustainability. In addition, ash mapping can contribute to fertilizers' variable rate applications, aiming to take advantage of the chemical elements already deposited by the ash [23]. In literature, few studies explore ash mapping in agriculture. In addition, the existing articles explore ash application from other sources. In coffee management, the previous crop biomass is burned on the ground, which makes the study even more specific. Ash management is still little explored in coffee farming, as we did not find articles related to this study.

Given this premise, monitoring regions with ash deposits is essential to know which elements are present on the ground after biomass burning. Additionally, it is important to know which elements are identified in conventional soil analysis and their possible interference with plant development. Therefore, this study aimed to evaluate (I) the chemical elements present in ash and their correlation with vegetative development after planting; (II) the performances of vegetative indices applied to areas mapping ash deposits; and (III) the temporal mapping of ash deposited after the renovation burning of coffee plantations by vegetative indices.

2. Materials and Methods

2.1. Study Area

The study region comprised an area of 8 hectares intended for coffee cultivation (Figure 1). It was in Santo Antônio do Amparo, Minas Gerais, Brazil, at the coordinates 21°00′55.55″S e 44°54′57.75″W. The regional climate is characterized as hot and temperate. The regional climate is warm and temperate, with annual average temperatures between 20 and 22 °C, yearly rainfall between 1300 and 1600 mm, and altitudes between 800 and 1000 m [24].

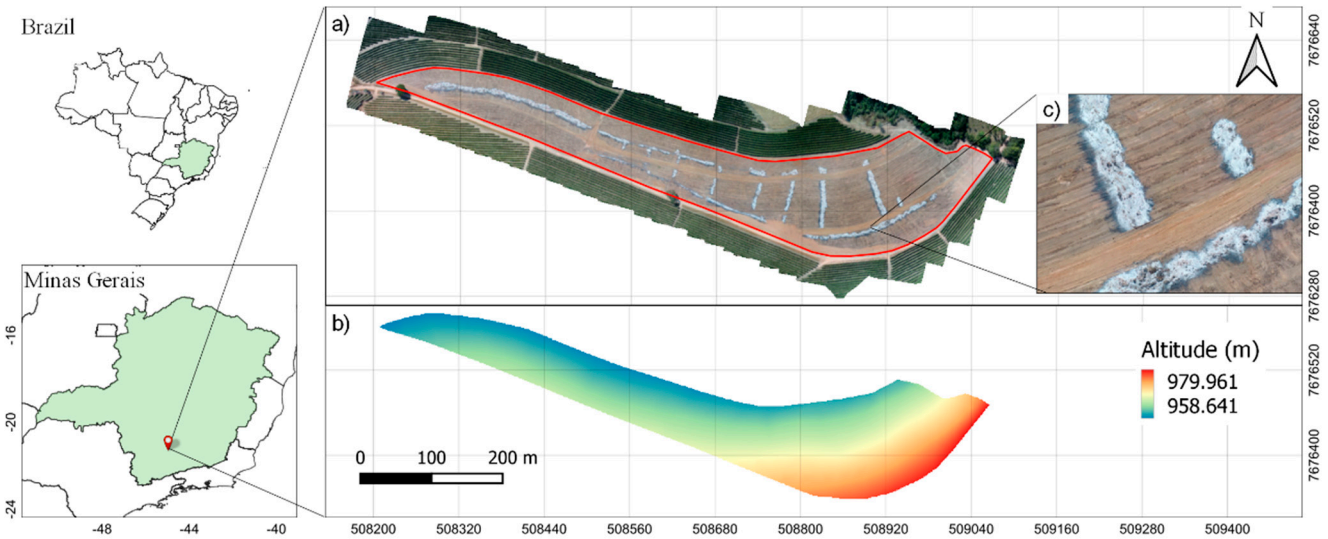


Figure 1. Study area. (**a**) Study area boundary (red), (**b**) digital terrain model (DTM), and (**c**) regions with ash deposits.

2.2. Field Data Collection

2.2.1. Soil Chemical Properties

Samples were taken in two distinct regions (natural soil and soil with ash present) at a depth of 0–0.20 m. The area was divided into three sampling blocks. Each block comprised six ash samples and six natural soil samples, totaling thirty-six samples (Figure 2).

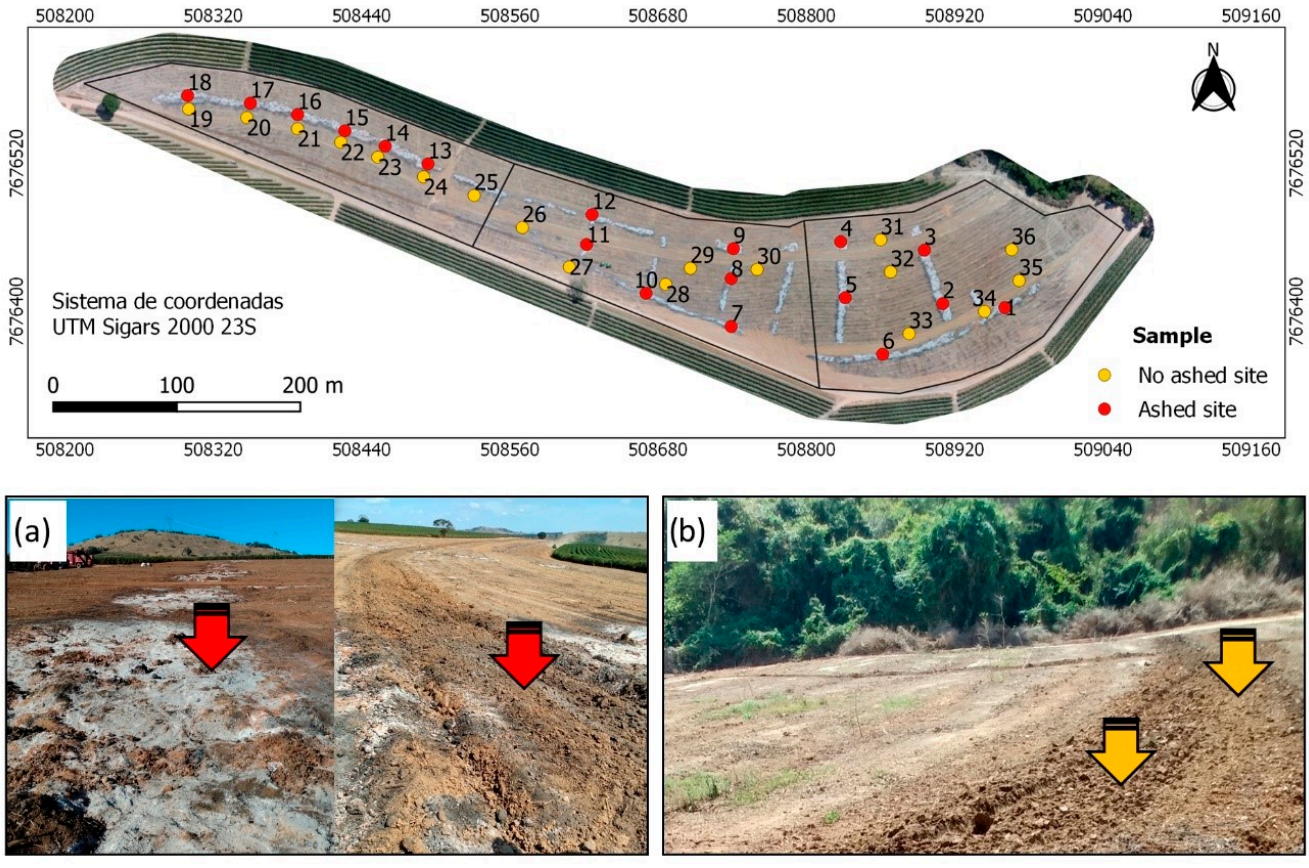


Figure 2. Sampling points map; (**a**) collection of samples in regions with ash deposits and (**b**) collection of samples in regions are ash-free.

The collected samples were sent to a soil analysis laboratory to determine Mg, Al, Ca, Mg, K, B, Zn, S, and P; cation exchange capacity (CEC); soil pH; organic matter; and base saturation. These results were subjected to statistical analysis to verify the degree of interference of ash deposits on soil nutrient availability.

2.2.2. Chemical Analysis of Ash

The ash was collected in the previously mapped locations. Two samples were collected, composed of six subsamples of pure ash, and then taken to the laboratory, where they were subjected to chemical analysis. After a multi-acid digestion process (hydrofluoric acid, perchloric acid, hydrochloric acid, and nitric acid), the materials were analyzed by inductively coupled plasma atomic emission spectrometry (ICP–OES). This analysis can quantify the presence of the following elements: Ag, Al, As, Ba, Be, Bi, Ca, Cd, Co, Cr, Cu, Fe, Ga, Gd, K, La, Li, Mg, Mn, Mo, Na, Ni, P, Pb, S, Sb, Sc, Se, Sn, Sr, Th, Tl, Ti, U, V, W, Y, and Zn.

2.2.3. Photogrammetric Data Collection

Photogrammetric data were collected at one, four, and six months after planting coffee. The images were collected by a Matrice 100 Remotely Piloted Aircraft RPA (DJI, Shenzhen, China) (Figure 3a). A quadcopter weighing 2431 g and that was 600 mm in horizontal length, with a flight capacity of 20 min, 500 g payload, and 2 km distance from the radio control, was used. This RPA was equipped with a sequoia camera (Figure 3b). The collected images were used to determine the vegetative indices (VIs).

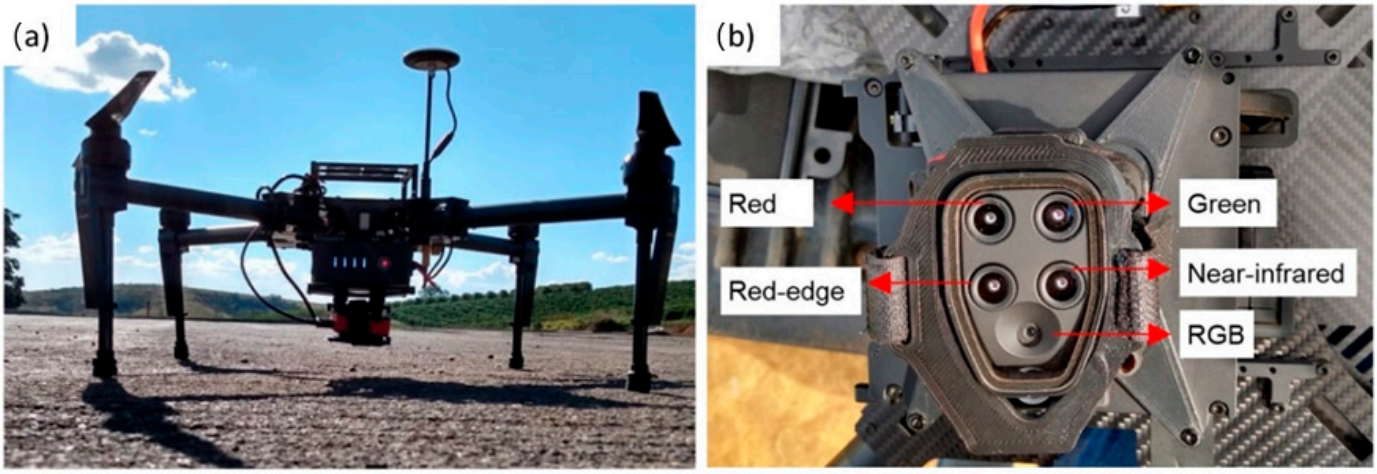


Figure 3. (**a**) Remotely Piloted Aircraft DJI Matrice 100, (**b**) Parrot Sequoia multispectral camera.

The Sequoia sensor (Figure 3b) had a high-resolution RGB camera with a 4608 × 3456-pixel sensor, 1.34 µm pixel size, and 4.88 mm focal length; the ground sampling distance (GSD) was from 1.9 cm to 70 m above ground level (AGL). In addition, four monochromatic cameras were sensitive to the following spectral bands: green (G, 530–570 nm), red (R, 640–680 nm), red edge (RE, 730–740 nm), and near-infrared (NIR, 77–810 nm). These sensors featured a resolution of 1280 × 960 pixels, a pixel size of 3.75 µm, and a focal length of 3.98 mm; the GSD was 6.8 cm at a 70 m flight height (AGL) [25].

Before starting the flights, safety factors were observed, highlighting weather conditions, wind speed, presence of objects, poles, trees, and electrical transmission towers. Flight planning was performed using the Precision Flight software (Version 1.3.2, Precision Hawk, Raleigh, NC, USA). The input parameters were added considering better flight efficiency, reduced numbers of turns made by the aircraft, and adequate places for landing and take-off. Thus, the flight characteristics were 90 m (AGL), the frontal and lateral overlap of the images was 80 × 80%, and the flight speed was 6 m/s.

All flights were carried out between 10:00 am and 1:00 pm to reduce shading interference. In addition, the image capture was complemented by radiometric sensor calibration, achieved by accurately compensating for incident light conditions and generating quantitative data on a calibration (reference) plate to capture images according to variations in sunlight during flight.

2.3. Image Processing

The collected images were processed in the software PIX4Dmapper version 4.4.12 (Pix4D, Lausanne, Switzerland). This software has an algorithm based on Structure-from-Motion (SfM). SfM approaches can be considered superior in accuracy when the user intends to generate orthomosaic and DTM [26,27]. In addition, they contain computer vision techniques that enable photogrammetry algorithms that achieve high-precision processing on aerial images [28].

The standard Pix4Dmapper "Ag Multispectral" model was used to generate the orthomosaics of individual spectral bands (green, red, red edge, and near-infrared). The images were georeferenced using control points previously collected in the field area by a differential GNSS (Trimble Navigation Limited, Sunnyvale, CA, USA) model SP 60 of spectrum precision, with a vertical precision of 0.07 m to improve orthomosaic precision. After generating the orthomosaics, the vegetation indices were calculated in Pix4D and exported with the TIFF extension for further analysis.

Vegetation Indices

Vegetation indices (VIs) are fundamental measurements in coffee plant vegetative development analysis [29,30]. Thirty-one vegetation indices (Table 1) were selected based on the Index Database [31] to find the best index for mapping the ash. The vegetation indices associated with Parrot Sequoia camera spectral bands were considered. Then, the indices were calculated in images of coffee trees four, six, and ten months after implantation.

Table 1. Vegetation indices of multispectral images obtained using RPA. R: red band; G: green band; NIR: near infrared band; RE: red edge band.

Index	Equation
Normalized Green Index (NGI)	$G/(NIR + RE + G)$
Normalized Red Edge Index (NREI)	$RE/(NIR + RE + G)$
Normalized Red Index (NRI)	$R/(NIR + RE + R)$
Normalized NIR Index (NNIR)	$NIR/(NIR + RE + G)$
Modified Double Difference Index (MDD)	$(NIR - RE) - (RE - G)$
Modified Normalized Difference Index (MNDI)	$\frac{(NIR-RE)}{(NIR-G)}$
Modified Enhanced Vegetation Index (MEVI)	$\frac{2.5\times(NIR-RE)}{(NIR+6\times RE-7.5\times G+1)}$
Modified Normalized Difference Red Edge (MNDRE)	$\frac{[NIR-(RE-2\times G)]}{[NIR+(RE-2\times G)]}$
Normalized Difference Vegetation Index (NDVI)	$\frac{(NIR-R)}{(NIR+R)}$
Modified Red Edge Transformed Vegetation Index (MRETVI)	$1.44 \times ((NIR - R) - 2.5 \times (RE - R))$
Red Edge Ratio Vegetation Index (RERVI)	$\frac{NIR}{RE}$
Red Edge Difference Vegetation Index (REDVI)	$NIR - RE$
Red Edge Renormalized Different Vegetation Index (RERDVI)	$\frac{(NIR-RE)}{\sqrt{NIR+RE}}$
Red Edge Wide Dynamic Range Vegetation Index (REWDRVI)	$\frac{(a\times NIR-RE)}{(a\times NIR+RE)} (a = 0.12)$
Red Edge Soil Adjusted Vegetation Index (RESAVI)	$1.5 \times \left[\frac{(NIR-RE)}{(NIR+RE+0.5)}\right]$
Red Edge Optimal Soil Adjusted Vegetation Index (REOSAVI)	$(1 + 0.16)(NIR - RE)/(NIR + RE + 0.16)$

Table 1. *Cont.*

Index	Equation
Modified Red Edge Soil Adjusted Vegetation Index (MRESAVI)	$0.5 \times \left[2 \times \mathrm{NIR} + 1 - \sqrt{(2 \times \mathrm{NIR} + 1)2 - 8 \times (\mathrm{NIR} - \mathrm{RE})}\right]$
Optimized Red Edge Vegetation Index (REVIopt)	$100 \times (\mathrm{lnNIR} - \mathrm{lnRE})$
Red Edge Chlorophyll Index (CIre)	$\mathrm{NIR}/\mathrm{RE} - 1$
Modified Red Edge Simple Ratio (MSR_RE)	$\frac{(\mathrm{NIR}/\mathrm{RE} - 1)}{\sqrt{(\mathrm{NIR}/\mathrm{RE} + 1)}}$
Red Edge Normalized Difference Vegetation Index (RENDVI)	$\frac{(\mathrm{RE} - \mathrm{R})}{(\mathrm{RE} + \mathrm{R})}$
Red Edge Simple Ratio (RESR)	RE/R
Modified Red Edge Difference Vegetation Index (MREDVI)	$\mathrm{RE} - \mathrm{R}$
DATT Index (DATT)	$(\mathrm{NIR} - \mathrm{RE})/(\mathrm{NIR} - \mathrm{R})$
Normalized Near Infrared Index (NNIRI)	$\mathrm{NIR}/(\mathrm{NIR} + \mathrm{RE} + \mathrm{R})$
Modified Transformed Chlorophyll Absorption In Reflectance Index (MTCARI)	$3 \times \left[(\mathrm{NIR} - \mathrm{RE}) - 0.2 \times (\mathrm{NIR} - \mathrm{R})\left(\frac{\mathrm{NIR}}{\mathrm{RE}}\right)\right]$
Modified Red Edge Simple Ratio (MRESR)	$(\mathrm{NIR} - \mathrm{R})/(\mathrm{RE} - \mathrm{R})$
Modified Normalized Difference Red Edge (MNDRE2)	$\frac{(\mathrm{NIR} - \mathrm{RE} + 2 * \mathrm{R})}{(\mathrm{NIR} + \mathrm{RE} - 2 * \mathrm{R})}$
Red Edge Transformed Vegetation Index (RETVI)	$0.5 \times [120 \times (\mathrm{NIR} - \mathrm{R}) - 200 \times (\mathrm{RE} - \mathrm{R})]$
NDVI (normalized difference vegetation index)	$\frac{(\mathrm{NIR} - \mathrm{R})}{(\mathrm{NIR} + \mathrm{R})}$
MTCI (terrestrial chlorophyll index)	$\frac{\mathrm{NIR} - \mathrm{RE}}{\mathrm{RE} + \mathrm{R}}$
Normalized difference red edge (NDRE)	$\frac{\mathrm{NIR} - \mathrm{RE}}{\mathrm{NIR} + \mathrm{RE}}$

Vegetation indices were processed in Rstudio 1.4 and QGIS software 3.28.7 to understand plant development in regions with ash deposits and in naturally cultivated soils. The index images were cut and separated into areas with ash (Ash–on) and areas that were ash-free (Ash-off) to understand the ash's direct effect on plants. Then, seven samples were collected in the vegetative indices at the same soil collection points, soil with ash regions and ash free-soil, using a 0.25 m buffer in each plant, totaling 126 samples for each variable. Thus, 31 index values evaluated for each identified region were obtained.

2.4. Statistical Analysis

Soil analysis data were statistically analyzed and expressed as an average in each treatment to indicate ash effects on the soil. In this analysis, SISVAR 5.6 software was used. Then, data normality was verified before starting the exploratory analysis (descriptive statistics). A "one-way" analysis of variance (ANOVA) was performed after normality verification. The F test was used, followed by the mean test (Tukey with 5% error probability). This proportional analysis statistically verified the interference of ash on soil nutrients by conventional samples.

The vegetative indices were evaluated by applying means tests to verify significant differences between plants located inside (Ash-on) and outside (Ash-off) the ash areas. For this, the Anderson–Darling test initially verified data normality [32]. Thus, for data with normal distribution, the multiple comparisons T-test was applied at 5% ($p < 0.05$) probability, and for data without normal distribution, the multiple comparisons Wilcoxon test at 5% ($p < 0.05$) probability was applied. All procedures were performed using RStudio software 1.4 (R Development Core Team, R project, New Zealand).

Crossing information from soil samples and mapping by RPAs can generate confusion in reproducing methods. The methodological steps are presented in Figure 4.

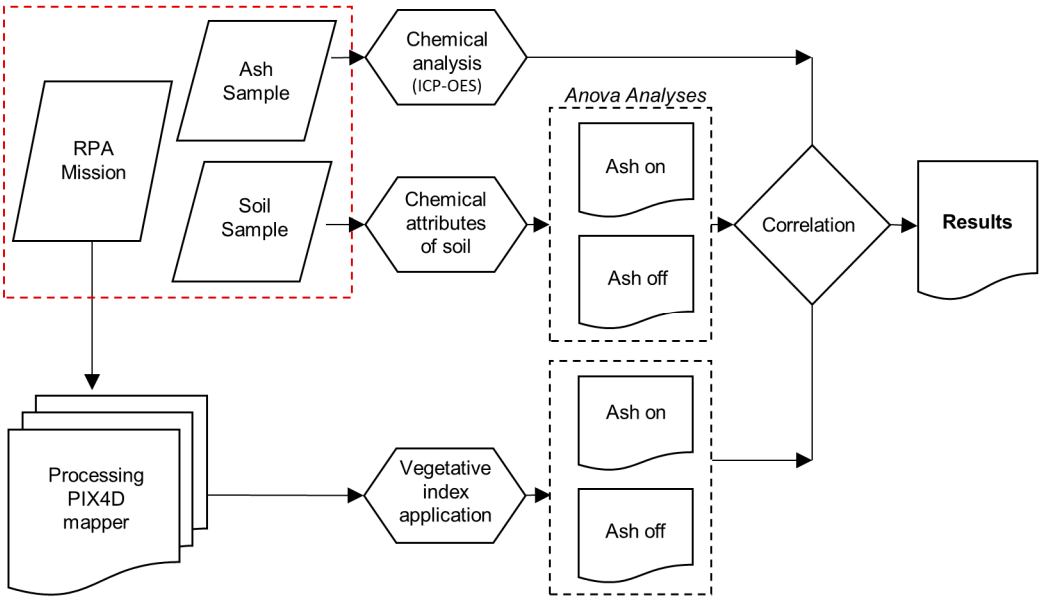


Figure 4. Flowchart for carrying out ash influences analysis on coffee trees.

The best indices were selected after statistical analysis. The criterion adopted was the index that presented significant differences in the mean tests. Then, a Pearson correction was applied to the data with ash and with ash-free soil, so the lowest correlations corresponded to the best vegetative indices.

3. Results

3.1. Ash Analysis

Pure ash analyses were essential to determine which nutrients were deposited on the soil after the plant remains were burned from the previous crop. Table 2 presents the inductively coupled plasma atomic emission spectrometry (ICP–OES) analysis results. Although the analysis results provided 41 chemical elements, the table shows quantitative results above the lower detection limit.

Table 2. Chemical elements present in pure ash by elemental analysis (ICP-OES).

Analyte	Al	Ca	Cr	Cu	Fe	K	Mg	Mn	Na	Ni	S	Ti	Zn
Unity	%	%	ppm	%	%	%	%	%	%	ppm	%	%	%
Amount	2.48	13.71	28	0.037	0.99	11.32	2.85	0.08	0.01	13	0.09	0.08	0.011

The elements found in ash agree with research already in literature, evidencing the notable presence of K, Mg, Ca, and Al. The study in [33] demonstrated the potential of nutrient incorporation in arable soils by showing a high presence of K and Mg.

Ash deposits on the ground can also provide an unwanted element for cultivation, which is aluminum (Al) addition. As shown in Table 2, ash was composed of 2.48% Al. Aluminum is known to restrict root growth, making plants inefficient at absorbing nutrients and water. In addition, it can inhibit the microbial processes involved in the soil–plant relationship [34].

3.2. Soil Analysis

Ash's effects on the changes in the percentage of soil nutrients are presented in average values, according to Tukey's tests (Figure 5).

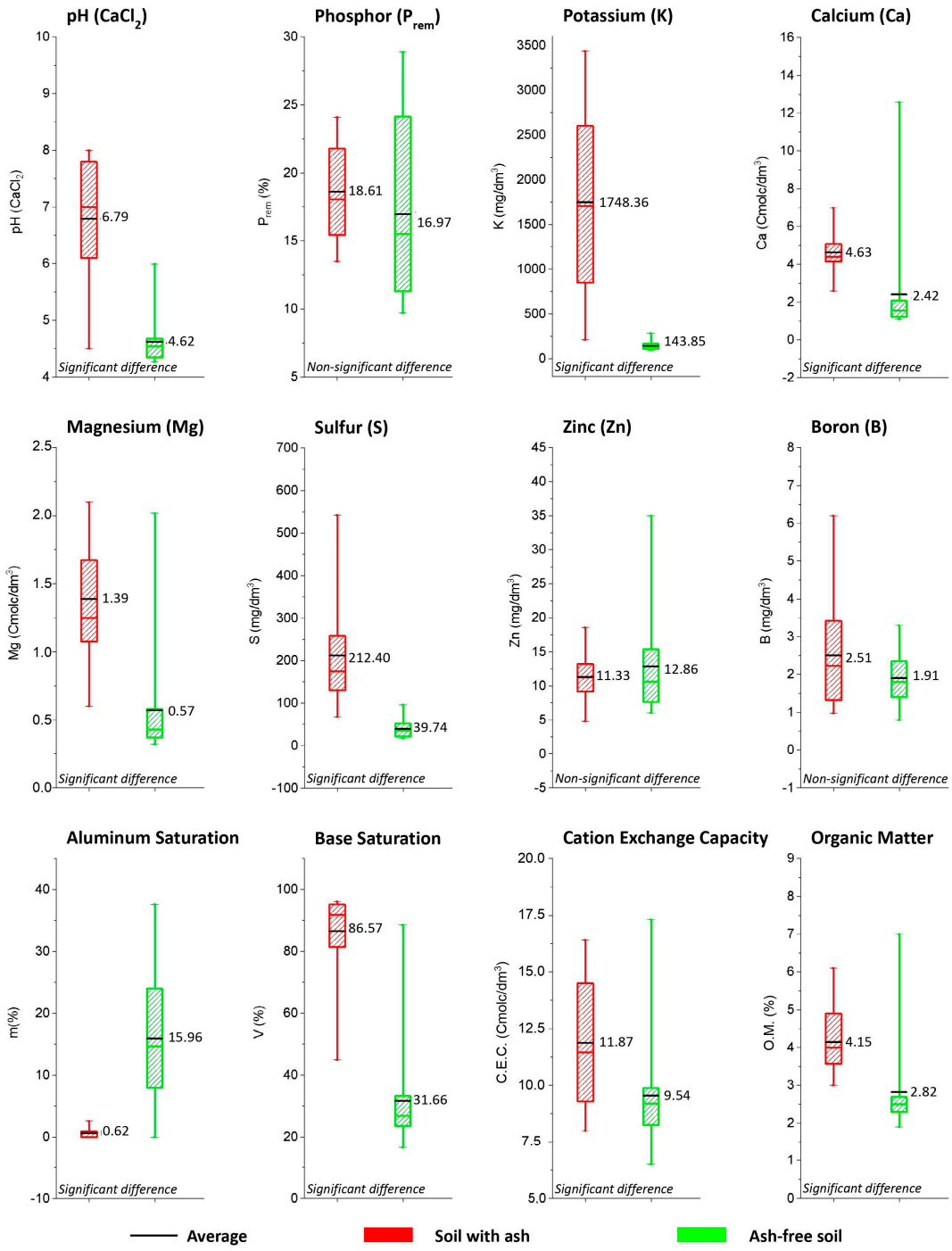


Figure 5. Results analysis of average tests of soil chemical attributes obtained by the Tukey test at a 5% error.

The information presented in Figure 5 shows significant differences between some important elements for plant development. In addition, the parameters obtained can be used for fertilization recommendations in coffee-growing management. A fact to be highlighted in the soil analysis is Al value inversion. In this analysis, the most significant presence of aluminum was in areas with ash-free soil. One hypothesis for this occurrence is high-temperature action in soil, modifying aluminum $Al_2(OH)_3$ to Al_2O_3.

On some coffee farms, burning plant biomass is used for the renewal of cultivation. This practice provides essential nutrients for plant development, but how ash is distributed in the field can cause an excess or deficiency of some nutrients. Figure 6 shows the coffee

plant's characteristics in regions with ash deposits. This imbalance may have occurred because the heaped material for burning accumulated at specific points in the field, depositing a significant amount of nutrients, such as K, Ca, and Mg (Figure 5).



Figure 6. Coffee plants four months after planting in regions with ash deposits.

As shown in Figure 6, coffee plants are affected by nutrient imbalances. Moyin-Jesu [35] explained that high K/Ca and K/Mg ratios present in the soil before fertilization influence treatment with NPK fertilization. This leads to an imbalance in the nutrient supply of K, Ca, and Mg to the coffee crop. For better use of these nutrients by plants, precision coffee-growing techniques are necessary. The postburn areas are treated as homogeneous in conventional coffee-growing area management. Figure 5 shows the differences between the Ash-on and Ash-off areas, especially with pH, K, Ca, Mg, and Al. Therefore, knowledge about the presence of nutrients in ash deposits after burning and inferences about significant differences in coffee plantations can be explored in precision coffee-growing techniques.

3.3. Vegetative Indices Analysis

The vegetative index application demonstrates class variations over time. Vegetative indices were applied at three development dates, but significant differences were observed only four months after coffee planting. The means tests applied for the first and sixth months after planting did not present significant results. In these stages of plant development, the indices did not differentiate plants in regions inside and outside the ash deposits. Therefore, vegetation index studies for plants inside and outside the ash area are presented only for plants four months after planting. The results are shown via boxplots with statistically significant differentiation by mean tests (Figure 7). Among the 31 indices tested for ash monitoring, only 20 showed significant differences, according to the means test.

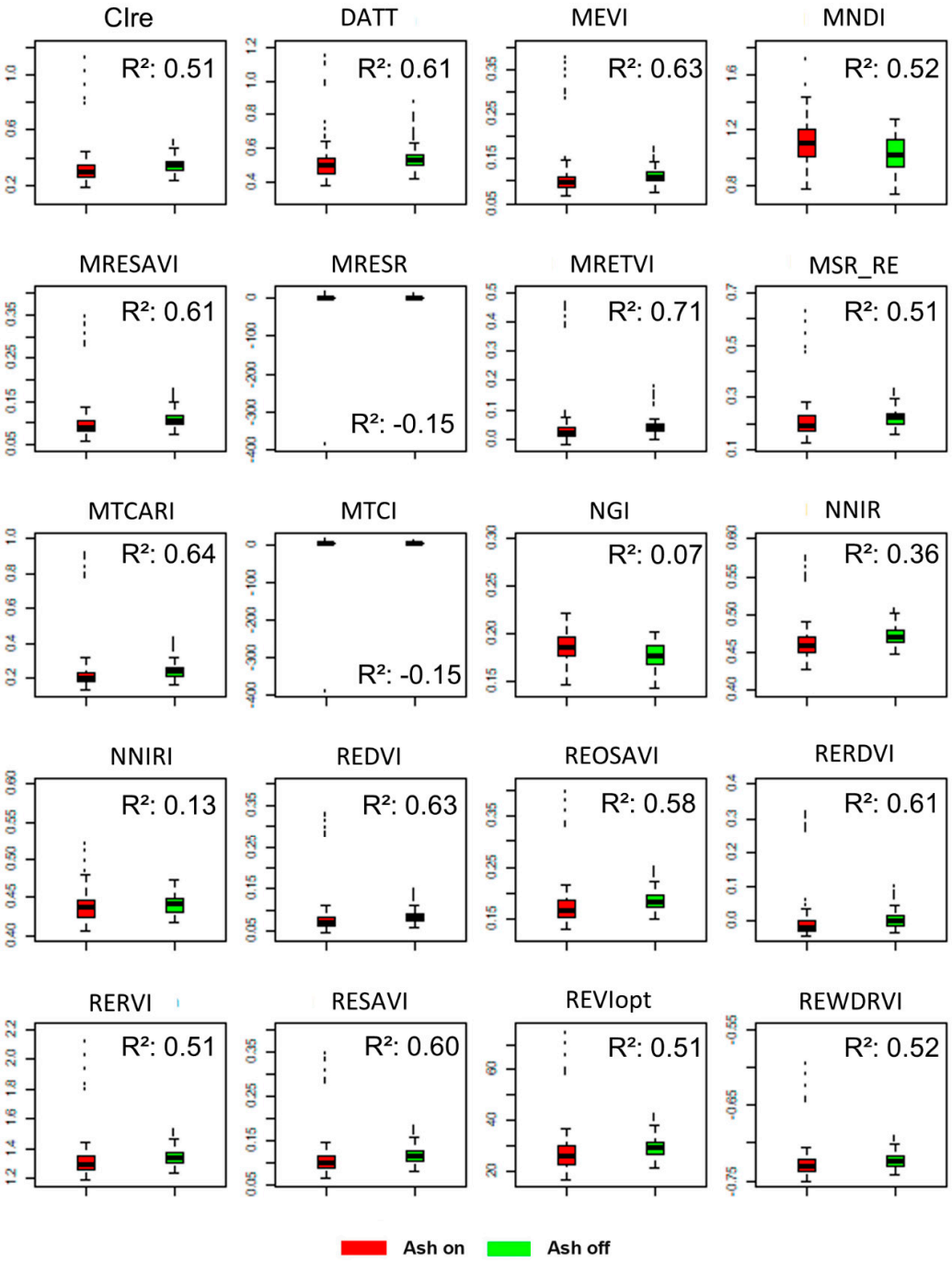


Figure 7. Vegetation indices with significant differences and the Pearson R^2 correlation between areas with ash and with ash-free soil in coffee plants within four months of planting.

4. Discussions

4.1. Ash Analysis

The aluminum toxicity level interferes with the availability, absorption, transport, and utilization of essential nutrients, such as phosphorus (P), potassium (K), calcium (Ca), magnesium (Mg), Fe, molybdenum (Mo), and boron (B) [36].

Soil chemical changes caused by ash on the surface can be confirmed in conventional soil chemical analyses. This is a point of fundamental importance, as this analysis generates essential information for recommendations on fertilization, liming, and other forms of soil management. In this research, it is possible to observe that pure ash's chemical elements can change the soil chemical composition.

4.2. Soil Analysis

Changes in aluminum form in the soil are evidenced in research by Certini [37]; fire causes changes in soil properties along a thermal gradient. Temperatures above 400 °C cause mineral transformation compounds, such as Al and Fe oxyhydroxides, and an approximately 600 °C thermal fusion of clay minerals can occur. Thus, the aluminum found in pure ash (Table 2) is probably in the Al_2O_3 form, since the burning process causes the aluminum to reach its maximum oxidation form. Al_2O_3 is a form of aluminum that does not harm plant development.

Some authors, such as Niu et al. [38]; Park et al. [39]; and Voundi Nkana [40] show the application of ash as promising for improvements in crop conditions. These studies mention the use of ash in agricultural areas, but they applied industrial ash from different burning processes. Biomass burning in the field can promote unexpected results for variations in chemical and physical parameters in the soil [41]. This occurrence may have affected the soil in the regions where the coffee biomass was burned.

The soil pH presented a significant difference (Figure 5). The pH is a primary soil variable, since it influences biological, chemical, and physical processes, affecting plant growth and biomass production [42]. Ash application is described in literature to increase the pH and deposition of macronutrients, such as K, Mg, and Ca [43]. Similar results are shown in Figure 5, highlighting greater variations for the K element; this occurrence is due to the organic matter of coffee residues containing N and K in their natural composition [44]. Ash has a beneficial effect as base fertilization and, mainly, as a cover. As a result of its chemical composition of slow solubilization of macro- and micronutrients, it can be compared to an NPK formula with a ratio of 1:3:7, in addition to Ca, Mg, and micronutrients [45].

4.3. Vegetative Indices Analysis

In coffee plantations, high plant similarity in the initial development makes it impossible to identify some anomalies. In this way, the first month's evaluation can be understood, as the index finds it challenging to differentiate plants in ash regions. In the initial development stage, the plant is in a transition phase; in some cases, it still uses nutrients present in the substrate [46]. Difficulties in evaluating the early stages of coffee plants were also evidenced in studies by Bento et al. [6], who applied vegetative indices to differentiate the development of cultivars after planting. The authors demonstrated low-density interference leaves for the vegetative index performance in the first months after planting.

The analysis presented in Figure 7 demonstrates that vegetative indices with low correlations between Ash-on and Ash-off areas can be considered the best ones to differentiate these areas. As shown in Figure 7, the Normalized Near Infrared Index (NNIRI) and Normalized Green Index (NGI) present the best R^2 results: 0.13 and 0.07, respectively. NGI index application was demonstrated in the research by Garba et al. [47], evidencing the ability to differentiate pasture growth at different stages, with green band presence in the NGI and NNIRI indices pointing to changes in the chlorophyll. According to Gitelson et al. [48], bands selected in GREEN, RED, and RE presented chlorophyll absorption features that can be used to determine the content of leaf chlorophyll with the modified chlorophyll absorption reflectance index. Analyzing Figure 6, it is possible to observe that changes in leaf color in regions with ash deposits correlate with better vegetative index performance using the green band.

Twenty vegetative indices performances presented fair values for monitoring plants in ash areas. However, the limitations of some VIs are related to the proximity between the average values obtained at the sampling points, which makes it challenging to map the effects of ash on plant development. Despite providing nutrients to the plants, the ash deposits present an uneven distribution, even within the contoured area. In addition, at some sampling points, nutrients may have been lost through leaching and surface transport. The best way to take advantage of these nutrients is to incorporate them into the soil after burning.

The uneven distribution of ash in the field interferes with the performance of vegetative indices. Additionally, it interferes with the spectral response, reducing vegetative indices efficiency created by multispectral images. Plant development characteristics may also have contributed to the low performances of some indices. Notably, the analyzed plants' ages may have influenced the correct performances of the vegetative indices. Sivanpillai and Booth [49] showed that a low amount of biomass drives similar spectral responses, impairing, in some cases, the analysis by vegetative indices.

The best vegetative index identification for ash monitoring offers the opportunity to carry out mapping throughout the study area. In Figure 8, the vegetative indices NGI and NNIRI were applied for monitoring four months after the coffee plantation. Figure 8a shows the mapping using RGB images before culture installation. The RGB mapping highlights the importance of mapping soon after the biomass is burned because, over time, the ash disappears from the surface, making it difficult to locate regions with ash. Figure 8b,c shows the best indices for ash monitoring among the 31 initially selected. In applying the indices to the total area, it is observed that some points were harmed, explained mainly by the surface runoff, causing ash accumulation and an increase in index values.

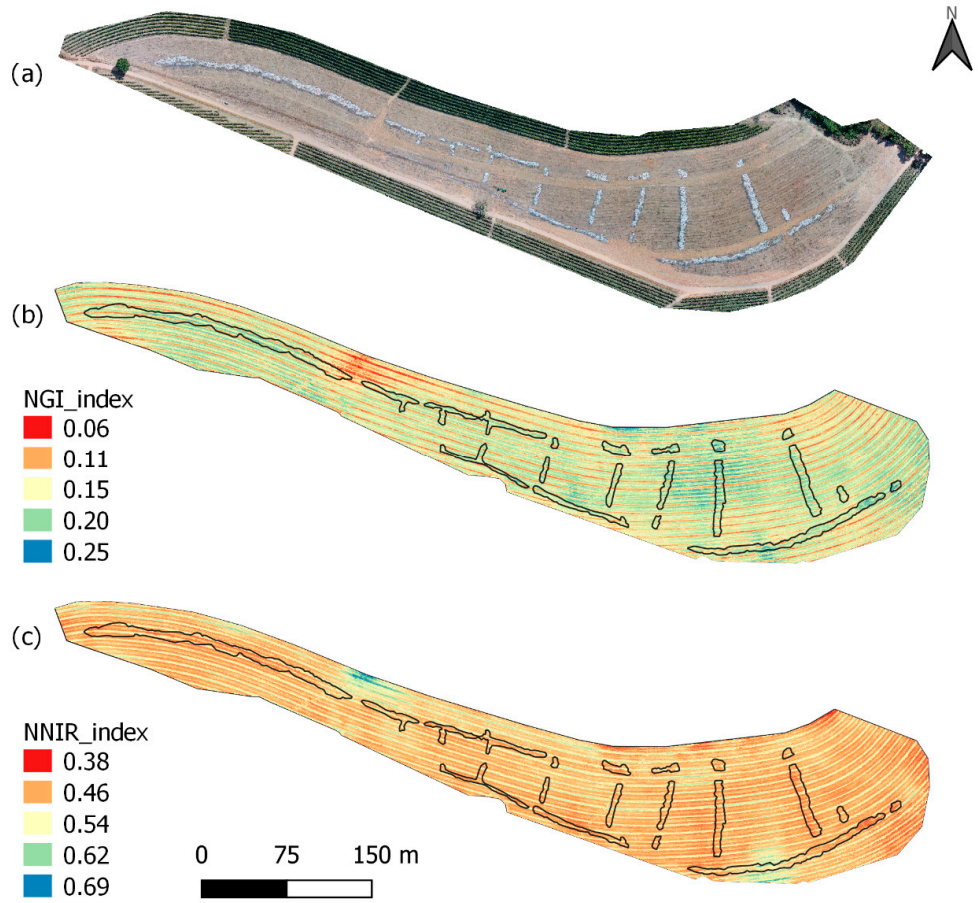


Figure 8. Monitoring by NGI and NNIRI indices in coffee plants with four months of planting: (**a**) ash location (RGB), (**b**) NGI index, and (**c**) NNIRI index.

Evaluation assertiveness by indices was positive only in the third month after planting. This was probably due to nutrient vulnerability losses soon after burning, since they were not incorporated into the soil. Nutrient-deposited vulnerability by ash on the surface is intensified by natural variables, such as precipitation, wind, and soil. Over time, the disappearance of points affected by ash can be influenced by rainfall, causing a leaching effect, carrying some nutrients and mixing with the soil. Thomaz et al. [50] reported ash's temporal effect on the soil and indicated that K is rapidly transferred from the ash to the

soil after repeated rainfall. In contrast, ash with Mg content is gradually leached into the soil, while Ca and P are leached even more slowly.

5. Conclusions

Plant residue burning in the field promoted the modification of Al present in the soil; then, the ash deposits on the soil raised the pH and added essential elements for plant development, such as K, Mg, and Ca.

The best indices for mapping plants in ash regions were the Normalized NIR Index (NNIRI) and Normalized Green Index (NGI) for plants four months after planting. The performances of these indices indicate that the monitoring of areas with ash should be guided in monitoring variations in chlorophyll.

Previous ash mapping can contribute to the realization of variable application in elements such as K and limestone. Vegetative indices can only be applied after four months of coffee development.

Author Contributions: Conceptualization, L.S.S. and G.A.e.S.F.; methodology, N.L.B. and L.S.S.; validation, G.A.e.S.F., M.S.S. and N.L.B.; formal analysis, J.M.d.S.; investigation, R.d.O.F.; resources, M.S.S.; data curation, J.M.d.S.; writing—original draft preparation, L.S.S. and M.S.S.; writing—review and editing, R.d.O.F.; visualization, R.d.O.F.; supervision, G.A.e.S.F.; project administration, G.A.e.S.F.; funding acquisition, G.A.e.S.F. All authors have read and agreed to the published version of the manuscript.

Funding: This research was funded by the EMBRAPA Café—Coffee Research Consortium, project no. 10.18.20.041.00.00, by the National Council for Scientific and Technological Development (CNPq), project no. 310186/2023-4, and by The Minas Gerais State Research Support Foundation (FAPEMIG) project no. APQ-00661-22.

Data Availability Statement: The data presented in this study are available on request from the corresponding author.

Acknowledgments: The authors express their gratitude to the Minas Gerais State Research Support Foundation (FAPEMIG), Bom Jardim Farm, Department of Agricultural Engineering and Federal University of Lavras for their administrative and technical assistance.

Conflicts of Interest: The authors declare no conflicts of interest.

References

1. Belan, L.L.; de Jesus Junior, W.C.; de Souza, A.F.; Zambolim, L.; Filho, J.C.; Barbosa, D.H.S.G.; Moraes, W.B. Management of Coffee Leaf Rust in Coffea Canephora Based on Disease Monitoring Reduces Fungicide Use and Management Cost. *Eur. J. Plant Pathol.* **2020**, *156*, 683–694. [CrossRef]
2. Vegro, C.L.R.; de Almeida, L.F. Global Coffee Market: Socio-Economic and Cultural Dynamics. In *Coffee Consumption and Industry Strategies in Brazil: A Volume in the Consumer Science and Strategic Marketing Series*; Elsevier: Amsterdam, The Netherlands, 2020; pp. 3–19, ISBN 9780128147214.
3. Paccioretti, P.; Córdoba, M.; Balzarini, M. FastMapping: Software to Create Field Maps and Identify Management Zones in Precision Agriculture. *Comput. Electron. Agric.* **2020**, *175*, 105556. [CrossRef]
4. Sarri, D.; Martelloni, L.; Rimediotti, M.; Lisci, R.; Lombardo, S.; Vieri, M. Testing a Multi-Rotor Unmanned Aerial Vehicle for Spray Application in High Slope Terraced Vineyard. *J. Agric. Eng.* **2019**, *50*, 38–47. [CrossRef]
5. Barbosa, B.D.S.; Ferraz, G.A.E.S.; Dos Santos, L.M.; Santana, L.S.; Marin, D.B.; Rossi, G.; Conti, L. Application of Rgb Images Obtained by Uav in Coffee Farming. *Remote Sens.* **2021**, *13*, 2397. [CrossRef]
6. Bento, N.L.; Ferraz, G.A.E.S.; Barata, R.A.P.; Soares, D.V.; dos Santos, L.M.; Santana, L.S.; Ferraz, P.F.P.; Conti, L.; Palchetti, E. Characterization of Recently Planted Coffee Cultivars from Vegetation Indices Obtained by a Remotely Piloted Aircraft System. *Sustainability* **2022**, *14*, 1446. [CrossRef]
7. Marin, D.B.; Ferraz, G.A.e.S.; Santana, L.S.; Barbosa, B.D.S.; Barata, R.A.P.; Osco, L.P.; Ramos, A.P.M.; Guimarães, P.H.S. Detecting Coffee Leaf Rust with UAV-Based Vegetation Indices and Decision Tree Machine Learning Models. *Comput. Electron. Agric.* **2021**, *190*, 106476. [CrossRef]
8. Chemura, A.; Mutanga, O.; Dube, T. Remote Sensing Leaf Water Stress in Coffee (Coffea Arabica) Using Secondary Effects of Water Absorption and Random Forests. *Phys. Chem. Earth* **2017**, *100*, 317–324. [CrossRef]
9. Putra, B.T.W.; Soni, P.; Marhaenanto, B.; Harsono, S.S.; Fountas, S. Using Information from Images for Plantation Monitoring: A Review of Solutions for Smallholders. *Inf. Process. Agric.* **2020**, *7*, 109–119. [CrossRef]

10. Marin, D.B.; Ferraz, G.A.e.S.; Schwerz, F.; Barata, R.A.P.; Faria, R.d.O.; Dias, J.E.L. Unmanned Aerial Vehicle to Evaluate Frost Damage in Coffee Plants. *Precis. Agric.* **2021**, *22*, 1845–1860. [CrossRef]
11. dos Santos, L.M.; Ferraz, G.A.e.S.; Barbosa, B.D.d.S.; Diotto, A.V.; Maciel, D.T.; Xavier, L.A.G. Biophysical Parameters of Coffee Crop Estimated by UAV RGB Images. *Precis. Agric.* **2020**, *21*, 1227–1241. [CrossRef]
12. Velásquez, D.; Sánchez, A.; Sarmiento, S.; Toro, M.; Maiza, M.; Sierra, B. A Method for Detecting Coffee Leaf Rust through Wireless Sensor Networks, Remote Sensing, and Deep Learning: Case Study of the Caturra Variety in Colombia. *Appl. Sci.* **2020**, *10*, 697. [CrossRef]
13. Ahmad, A.; Ordoñez, J.; Cartujo, P.; Martos, V. Remotely Piloted Aircraft (RPA) in Agriculture: A Pursuit of Sustainability. *Agronomy* **2020**, *11*, 7. [CrossRef]
14. Ronchetti, G.; Mayer, A.; Facchi, A.; Ortuani, B.; Sona, G. Crop Row Detection through RPAS Surveys to Optimise On-Farm Irrigation Management. In Proceedings of the EGU General Assembly 2019, Vienna, Austria, 7–12 April 2019; Volume 21.
15. Ivushkin, K.; Bartholomeus, H.; Bregt, A.K.; Pulatov, A.; Franceschini, M.H.D.; Kramer, H.; van Loo, E.N.; Jaramillo Roman, V.; Finkers, R. UAV Based Soil Salinity Assessment of Cropland. *Geoderma* **2019**, *338*, 502–512. [CrossRef]
16. Sankey, J.B.; Sankey, T.T.; Li, J.; Ravi, S.; Wang, G.; Caster, J.; Kasprak, A. Quantifying Plant-Soil-Nutrient Dynamics in Rangelands: Fusion of UAV Hyperspectral-LiDAR, UAV Multispectral-Photogrammetry, and Ground-Based LiDAR-Digital Photography in a Shrub-Encroached Desert Grassland. *Remote Sens. Environ.* **2021**, *253*, 112223. [CrossRef]
17. Martins, J.A.C.; Nogueira, K.; Osco, L.P.; Gomes, F.D.G.; Furuya, D.E.G.; Gonçalves, W.N.; Sant'ana, D.A.; Ramos, A.P.M.; Liesenberg, V.; Dos Santos, J.A.; et al. Semantic Segmentation of Tree-Canopy in Urban Environment with Pixel-Wise Deep Learning. *Remote Sens.* **2021**, *13*, 3054. [CrossRef]
18. Zhang, Y.; Ghaly, A.E.; Li, B. Availability and Physical Properties of Residues from Major Agricultural Crops for Energy Conversion through Thermochemical Processes. *Am. J. Agric. Biol. Sci.* **2012**, *7*, 312–321. [CrossRef]
19. Shakya, A.; Agarwal, T. Poultry Litter Biochar: An Approach towards Poultry Litter Management—A Review. *Int. J. Curr. Microbiol. Appl. Sci.* **2017**, *6*, 2657–2668. [CrossRef]
20. Zhai, J.; Burke, I.T.; Stewart, D.I. Beneficial Management of Biomass Combustion Ashes. *Renew. Sustain. Energy Rev.* **2021**, *151*, 111555. [CrossRef]
21. Dong, D.; Wang, C.; Van Zwieten, L.; Wang, H.; Jiang, P.; Zhou, M.; Wu, W. An Effective Biochar-Based Slow-Release Fertilizer for Reducing Nitrogen Loss in Paddy Fields. *J. Soils Sediments* **2020**, *20*, 3027–3040. [CrossRef]
22. Prasad, S.; Singh, A.; Korres, N.E.; Rathore, D.; Sevda, S.; Pant, D. Sustainable Utilization of Crop Residues for Energy Generation: A Life Cycle Assessment (LCA) Perspective. *Bioresour. Technol.* **2020**, *303*, 122964. [CrossRef]
23. Chaturvedi, S.; Singh, S.V.; Dhyani, V.C.; Govindaraju, K.; Vinu, R.; Mandal, S. Characterization, Bioenergy Value, and Thermal Stability of Biochars Derived from Diverse Agriculture and Forestry Lignocellulosic Wastes. *Biomass Convers. Biorefin* **2023**, *13*, 879–892. [CrossRef]
24. Alvares, C.A.; Stape, J.L.; Sentelhas, P.C.; De Moraes Gonçalves, J.L.; Sparovek, G. Köppen's Climate Classification Map for Brazil. *Meteorol. Z.* **2013**, *22*, 711–728. [CrossRef] [PubMed]
25. Franzini, M.; Ronchetti, G.; Sona, G.; Casella, V. Geometric and Radiometric Consistency of Parrot Sequoia Multispectral Imagery for Precision Agriculture Applications. *Appl. Sci.* **2019**, *9*, 5314. [CrossRef]
26. Dietrich, J.T. Riverscape Mapping with Helicopter-Based Structure-from-Motion Photogrammetry. *Geomorphology* **2016**, *252*, 144–157. [CrossRef]
27. Sona, G.; Pinto, L.; Pagliari, D.; Passoni, D.; Gini, R. Experimental Analysis of Different Software Packages for Orientation and Digital Surface Modelling from UAV Images. *Earth Sci. Inf.* **2014**, *7*, 97–107. [CrossRef]
28. Ruzgiene, B.; Berteška, T.; Gečyte, S.; Jakubauskiene, E.; Aksamitauskas, V.Č. The Surface Modelling Based on UAV Photogrammetry and Qualitative Estimation. *Measurement* **2015**, *73*, 619–627. [CrossRef]
29. Hunt, E.; Hively, W.; McCarty, G.; Daughtry, C.; Forrestal, P.; Kratochvil, R.; Carr, J.; Allen, N.; Fox-Rabinovitz, J.; Miller, C. NIR-Green-Blue High-Resolution Digital Images for Assessment of Winter Cover Crop Biomass. *GIsci Remote Sens.* **2011**, *48*, 86–98. [CrossRef]
30. Nogueira, S.M.C.; Moreira, M.A.; Volpato, M.M.L. Relationship between Coffee Crop Productivity and Vegetation Indexes Derived from Oli/Landsat-8 Sensor Data with and without Topographic Correction. *Eng. Agric.* **2018**, *38*, 387–394. [CrossRef]
31. The IDB Project Index DataBase. A Database for Remote Sensing Indices. IDB Project, 2011–2019. Available online: https://www.indexdatabase.de/ (accessed on 27 May 2022).
32. Scholz, F.W.; Stephens, M.A. K-Sample Anderson–Darling Tests. *J. Am. Stat. Assoc.* **1987**, *82*, 918–924. [CrossRef]
33. Pandey, V.C.; Singh, N. Impact of Fly Ash Incorporation in Soil Systems. *Agric. Ecosyst. Environ.* **2010**, *136*, 16–27. [CrossRef]
34. Poschenrieder, C.; Gunsé, B.; Corrales, I.; Barceló, J. A Glance into Aluminum Toxicity and Resistance in Plants. *Sci. Total Environ.* **2008**, *400*, 356–368. [CrossRef] [PubMed]
35. Moyin-Jesu, E.I. Effect of Some Organic Fertilizers on Soil and Coffee (*Coffea Arabica* L.) Leaf Chemical Composition and Growth. *Univ. Khartoum J. Agric. Sci.* **2007**, *15*, 52–70.
36. Singh, S.; Tripathi, D.K.; Singh, S.; Sharma, S.; Dubey, N.K.; Chauhan, D.K.; Vaculík, M. Toxicity of Aluminium on Various Levels of Plant Cells and Organism: A Review. *Environ. Exp. Bot.* **2017**, *137*, 177–193. [CrossRef]
37. Certini, G. Effects of Fire on Properties of Forest Soils: A Review. *Oecologia* **2005**, *143*, 1–10. [CrossRef] [PubMed]

38. Niu, Y.; Tan, H.; Hui, S. Ash-Related Issues during Biomass Combustion: Alkali-Induced Slagging, Silicate Melt-Induced Slagging (Ash Fusion), Agglomeration, Corrosion, Ash Utilization, and Related Countermeasures. *Prog. Energy Combust. Sci.* **2016**, *52*, 1–61. [CrossRef]
39. Park, N.D.; Michael Rutherford, P.; Thring, R.W.; Helle, S.S. Wood Pellet Fly Ash and Bottom Ash as an Effective Liming Agent and Nutrient Source for Rye Grass (*Lolium Perenne* L.) and Oats (Avena Sativa). *Chemosphere* **2012**, *86*, 427–432. [CrossRef] [PubMed]
40. Voundi Nkana, J.C.; Demeyer, A.; Verloo, M.G. Effect of Wood Ash Application on Soil Solution Chemistry of Tropical Acid Soils: Incubation Study. *Bioresour. Tehcnology* **2002**, *85*, 323–325. [CrossRef] [PubMed]
41. Fontúrbel, T.; Carrera, N.; Vega, J.A.; Fernández, C. The Effect of Repeated Prescribed Burning on Soil Properties: A Review. *Forests* **2021**, *12*, 767. [CrossRef]
42. Minasny, B.; Hong, S.Y.; Hartemink, A.E.; Kim, Y.H.; Kang, S.S. Soil PH Increase under Paddy in South Korea between 2000 and 2012. *Agric Ecosyst Environ.* **2016**, *221*, 205–213. [CrossRef]
43. Ribeiro, J.P.; Vicente, E.D.; Gomes, A.P.; Nunes, M.I.; Alves, C.; Tarelho, L.A.C. Effect of Industrial and Domestic Ash from Biomass Combustion, and Spent Coffee Grounds, on Soil Fertility and Plant Growth: Experiments at Field Conditions. *Environ. Sci. Pollut. Res.* **2017**, *24*, 15270–15277. [CrossRef]
44. Kasongo, R.K.; Verdoodt, A.; Kanyankagote, P.; Baert, G.; Ranst, E. Van Coffee Waste as an Alternative Fertilizer with Soil Improving Properties for Sandy Soils in Humid Tropical Environments. *Soil Use Manag.* **2011**, *27*, 94–102. [CrossRef]
45. Nolasco, A.M.; Guerrini, I.A.; Benedetti, V.; Gonçalves, J.L.M. Uso de Resíduos Urbanos e Industriais Como Fonte de Nutrientes e Condicionadores de Solos Florestais. In Proceedings of the Simpósio sobre Fertilização e Nutrição Florestal, Piracicaba, Brazil, 1999.
46. Silva Vallone, H.; Guimarães, R.J.; Nazareno, A.; Mendes, G.; Alberto, C.; Souza, S.; Dias, F.P.; Carvalho, A.M. *Recipientes E Substratos Na Produção de Mudas E No Desenvolvimento Inicial de Cafeeiros Após o Plantio 1 Recipients and Substrates in the Production of Seedlings and Initial Development of Coffee Trees after Planting*; Editora da Universidade Federal de Lavras: Lavras, Brazil, 2009; Volume 33.
47. Garba, I.; Salifou, I.; Sallah, A.; Samba, A.; Toure, I.; Yapo, Y.; Agoumo, A.; Soumana, S.; Oumarou, A.; Tychon, B.; et al. Mapping of Zones at risk (ZAR) in west Africaby using NGI, VCI and SNDVI from the e-station. *Int. J. Adv. Res.* **2017**, *5*, 1377–1386. [CrossRef] [PubMed]
48. Gitelson, A.A.; Kaufman, Y.J.; Stark, R.; Rundquist, D. Novel Algorithms for Remote Estimation of Vegetation Fraction. *Remote Sens. Environ.* **2002**, *80*, 76–87. [CrossRef]
49. Sivanpillai, R.; Booth, D.T. Characterizing Rangeland Vegetation Using Landsat and 1-Mm VLSA Data in Central Wyoming (USA). *Agrofor. Syst.* **2008**, *73*, 55–64. [CrossRef]
50. Thomaz, E.L.; Antoneli, V.; Doerr, S.H. Effects of Fire on the Physicochemical Properties of Soil in a Slash-and-Burn Agriculture. *CATENA* **2014**, *122*, 209–215. [CrossRef]

Disclaimer/Publisher's Note: The statements, opinions and data contained in all publications are solely those of the individual author(s) and contributor(s) and not of MDPI and/or the editor(s). MDPI and/or the editor(s) disclaim responsibility for any injury to people or property resulting from any ideas, methods, instructions or products referred to in the content.